

Orbital Dzyaloshinskii-Moriya Exchange Interaction

Panjin Kim¹ and Jung Hoon Han^{1,2,*}

¹*Department of Physics and BK21 Physics Research Division,
Sungkyunkwan University, Suwon 440-746, Korea*

²*Asia Pacific Center for Theoretical Physics, POSTECH, Pohang, Gyeongbuk 790-784, Korea*
(Dated: November 9, 2018)

Superexchange calculation is performed for multi-orbital band models with broken inversion symmetry. Orbital-changing hopping terms allowed by the symmetry breaking electric field lead to a new kind of orbital exchange interaction closely resembling the Dzyaloshinskii-Moriya spin exchange. Inversion symmetry breaking as present in surfaces and interfaces and a strong on-site repulsion, but not the spin-orbit interaction, are the requirements to observe the proposed effect. Mean-field phase diagram exhibits a rich structure including anti-ferro-orbital, ferro-orbital, and both single and multiple spiral-orbital phases in close analogy with the Skyrmion spin crystal phase recently discovered in thin-film chiral magnets.

PACS numbers: 75.25.Dk, 75.30.Et, 75.10.Hk

I. INTRODUCTION

Strong on-site repulsion transforms the Bloch bands of nearly-free electrons into an insulator where the residual low-energy dynamics is that of the spin degrees of freedom interacting with each other via the superexchange mechanism¹. For spin-orbit-coupled bands, the spin-flip hopping processes result in another type of spin exchange called the Dzyaloshinskii-Moriya (DM) interaction² under the superexchange process. Symmetry-wise, local inversion symmetry breaking such as the bond distortion for a pair of adjacent magnetic orbitals, in addition to the spin-orbit interaction (SOI), is the pre-requisite for the DM interaction to make its appearance in a given system. Ordered magnetic ground state is modified from being collinear as a result of the DM exchange to favor spiral structure.

Meanwhile, inversion symmetry breaking (ISB) on the global scale takes place for surfaces and interfaces and affects the band structure with new effects such as the Rashba interaction³. The situation was recently reviewed carefully in Refs. 4,5 where it was shown that the symmetry-breaking electric field along the surface-normal z -direction modifies the band structure within the xy -plane by allowing previously forbidden hopping processes. Examples are $p_{x(y)} \leftrightarrow p_z$ orbital hopping in the p -band, and $d_{xy} \leftrightarrow d_{zx}$ orbital hopping in the t_{2g} -band. It was further shown⁵ that the new hopping terms arising from ISB can be cast in the form $-\gamma \sum_{\mathbf{k}} \Psi_{\mathbf{k}}^{\dagger} \mathbf{L} \cdot (\mathbf{k} \times \hat{z}) \Psi_{\mathbf{k}}$ around the Γ ($\mathbf{k} = 0$) point, where $\Psi_{\mathbf{k}}$ is the collection of, say, p -orbital operators $(X_{\mathbf{k}}, Y_{\mathbf{k}}, Z_{\mathbf{k}})^T$ in momentum coordinates \mathbf{k} , γ is a parameter measuring the degree of ISB, and \mathbf{L} is the spin-1 orbital angular momentum (OAM) operator. From the structure of the new Hamiltonian it readily follows that each band will carry polarized OAM proportional to $h(\mathbf{k} \times \hat{z})$ with the respective helicities $h = +1, 0, -1$ ⁵. The enlargement of effective spin size from 1/2 (as in electrons' spin) to 1 (as in degenerate p -orbital bands) results in the appearance of the third band that remains unpolarized. The chiral struc-

ture of the OAM, dubbed the ‘‘orbital Rashba effect’’, can occur even in the complete absence of SOI, and has been confirmed by circular dichroism ARPES work on the weak-SOI material, Cu⁶.

The new hopping processes allowed by ISB are in fact the orbital analogues of spin-flip hoppings in spin-orbit-coupled bands. Therefore, the two necessary conditions for the emergence of spin-DM interaction - ISB and SOI - are both effectively fulfilled for orbital magnetism when a symmetry-breaking electric field acts perpendicular to the two-dimensional surface. The purpose of this paper is to review this situation carefully in the limit of strong on-site interaction regime to ask if an orbital analogue of spin-DM interaction exists. In Sec. II superexchange calculation is carried out for multi-orbital tight-binding Hamiltonian embodying the ISB. The emergence of the orbital DM interaction is demonstrated in Sec. III together with the phase diagram exhibiting spiral and multi-spiral structures. Possible observation of orbital DM-induced orbital-spiral phases in magnetic thin films is discussed in Sec. IV.

II. SUPEREXCHANGE WITH ISB

Assuming three degenerate p -orbital states at each site, a square lattice Hamiltonian with nearest-neighbor hopping $H_t = \sum_{i\sigma} (H_{i,i+\hat{x},\sigma} + H_{i,i+\hat{y},\sigma})$ is constructed,

$$\begin{aligned} H_{i,i+\hat{x},\sigma} &= t_a X_{i\sigma}^{\dagger} X_{i+\hat{x},\sigma} + t_b [Y_{i\sigma}^{\dagger} Y_{i+\hat{x},\sigma} + Z_{i\sigma}^{\dagger} Z_{i+\hat{x},\sigma}] \\ &\quad + \gamma (X_{i\sigma}^{\dagger} Z_{i+\hat{x},\sigma} - Z_{i\sigma}^{\dagger} X_{i+\hat{x},\sigma}) + h.c. \\ H_{i,i+\hat{y},\sigma} &= t_a Y_{i\sigma}^{\dagger} Y_{i+\hat{y},\sigma} + t_b [X_{i\sigma}^{\dagger} X_{i+\hat{y},\sigma} + Z_{i\sigma}^{\dagger} Z_{i+\hat{y},\sigma}] \\ &\quad + \gamma (Y_{i\sigma}^{\dagger} Z_{i+\hat{y},\sigma} - Z_{i\sigma}^{\dagger} Y_{i+\hat{y},\sigma}) + h.c. \quad . \quad (1) \end{aligned}$$

Two hopping integrals t_a and t_b are introduced for σ - and π -bonding orbital hoppings, respectively. Inter-orbital hopping becomes possible when the ISB parameter γ is nonzero^{4,5}. All hopping parameters are real due to the assumed time-reversal invariance. Three-component spinor

can be formed, $\psi_i = (X_i \ Y_i \ Z_i)^T$, representing the p_x -, p_y -, and p_z -orbitals at the site i . Multi-orbital Hubbard interaction is⁷

$$H_U = U \sum_{i\alpha} n_{i\alpha\uparrow} n_{i\alpha\downarrow} + \left(U - \frac{5}{2} J_H \right) \sum_{i,\alpha < \beta, \sigma, \sigma'} n_{i\alpha\sigma} n_{i\beta\sigma'} - 2J_H \sum_{i,\alpha < \beta} \mathbf{S}_{i\alpha} \cdot \mathbf{S}_{i\beta} + J_H \sum_{i,\alpha \neq \beta} c_{i\alpha\uparrow}^\dagger c_{i\alpha\downarrow}^\dagger c_{i\beta\downarrow} c_{i\beta\uparrow}, \quad (2)$$

where U and J_H are Coulomb and Hund's exchange elements, α , β and σ , σ' are orbital and spin indices, respectively, and $n_{i\alpha\sigma}$ is a number operator counting the electron number in α -orbital with spin σ at site i .

Shekhtman *et al.* showed how to carry out the superexchange calculation efficiently for spin-orbit-coupled bands by introducing unitary rotations for operators to absorb spin-flip hoppings⁸. We may adopt similar unitary rotations, in the orbital subspace, to remove orbital-changing hoppings from the Hamiltonian (1) with two unitary matrices

$$U_x = \begin{pmatrix} \cos \frac{\theta}{2} & 0 & \sin \frac{\theta}{2} \\ 0 & 1 & 0 \\ -\sin \frac{\theta}{2} & 0 & \cos \frac{\theta}{2} \end{pmatrix}, \quad U_y = \begin{pmatrix} 1 & 0 & 0 \\ 0 & \cos \frac{\theta}{2} & \sin \frac{\theta}{2} \\ 0 & -\sin \frac{\theta}{2} & \cos \frac{\theta}{2} \end{pmatrix}. \quad (3)$$

Two distinct rotations are required since the orbital-changing hopping mixes (p_x, p_z) orbitals along the x -direction, but (p_y, p_z) orbitals for the y -direction. As the new operators

$$\begin{aligned} \tilde{\psi}_{i,x(y)} &= U_{x(y)}^\dagger \psi_i, \\ \tilde{\psi}_{i+\hat{x}} &= U_x \psi_{i+\hat{x}}, \\ \tilde{\psi}_{i+\hat{y}} &= U_y \psi_{i+\hat{y}} \end{aligned} \quad (4)$$

are inserted in Eq. (1) one obtains a new hopping Hamiltonian $\tilde{H}_t = \sum_{i\sigma} (\tilde{H}_{i,i+\hat{x},\sigma} + \tilde{H}_{i,i+\hat{y},\sigma})$,

$$\begin{aligned} \tilde{H}_{i,i+\hat{x},\sigma} &= (t+t_2) \tilde{X}_{i\sigma}^\dagger \tilde{X}_{i+\hat{x},\sigma} + t_b \tilde{Y}_{i\sigma}^\dagger \tilde{Y}_{i+\hat{x},\sigma} \\ &\quad + (t-t_2) \tilde{Z}_{i\sigma}^\dagger \tilde{Z}_{i+\hat{x},\sigma} + h.c. \\ \tilde{H}_{i,i+\hat{y},\sigma} &= t_b \tilde{X}_{i\sigma}^\dagger \tilde{X}_{i+\hat{x},\sigma} + (t+t_2) \tilde{Y}_{i\sigma}^\dagger \tilde{Y}_{i+\hat{x},\sigma} \\ &\quad + (t-t_2) \tilde{Z}_{i\sigma}^\dagger \tilde{Z}_{i+\hat{x},\sigma} + h.c., \end{aligned} \quad (5)$$

where $t(\cos \theta, \sin \theta) = (t_1, \gamma)$, $t_1 = (t_a + t_b)/2$, $t_2 = (t_a - t_b)/2$. Although bearing the same notation, the meaning of the tilde operators appearing in $\tilde{H}_{i,i+\hat{x},\sigma}$ is distinct from that in $\tilde{H}_{i,i+\hat{y},\sigma}$ due to different sets of rotations involved.

Superexchange calculation at 1/6-filling (one particle per site) can proceed now via standard methods with the Hamiltonian $H = \tilde{H}_t + H_U$, where the orbital-changing hopping terms are seemingly absent. The exchange Hamiltonian thus obtained, writing $t+t_2 \equiv t_{\tilde{x}}$, $t_b \equiv t_{\tilde{y}}$ and $t-t_2 \equiv t_{\tilde{z}}$, reads $\mathcal{H} = \mathcal{H}_{\tilde{x}} + \mathcal{H}_{\tilde{y}}$,

$$\begin{aligned} \mathcal{H}_{\tilde{x}} &= J_{T_1} \sum_i \left(\mathbf{S}_i \cdot \mathbf{S}_{i+\hat{x}} + \frac{3}{4} \right) \left(\hat{A}_{i,i+\hat{x}} + \hat{B}_{i,i+\hat{x}} - \hat{N}_{i,i+\hat{x}} \right) \\ &\quad + J_E \sum_i \left(\mathbf{S}_i \cdot \mathbf{S}_{i+\hat{x}} - \frac{1}{4} \right) \left(-\hat{A}_{i,i+\hat{x}} + \hat{B}_{i,i+\hat{x}} + \hat{N}_{i,i+\hat{x}} \right) \\ &\quad + J_{A_1} \sum_i \left(\mathbf{S}_i \cdot \mathbf{S}_{i+\hat{x}} - \frac{1}{4} \right) \left(\frac{2}{3} \hat{A}_{i,i+\hat{x}} + \frac{2}{3} \hat{C}_{i,i+\hat{x}} \right) \\ &\quad + J_{T_2} \sum_i \left(\mathbf{S}_i \cdot \mathbf{S}_{i+\hat{x}} - \frac{1}{4} \right) \left(\frac{4}{3} \hat{A}_{i,i+\hat{x}} - \frac{2}{3} \hat{C}_{i,i+\hat{x}} \right), \end{aligned} \quad (6)$$

where $J_{T_1} = 2/(U - 3J_H)$, $J_E = J_{T_2} = 2/(U - J_H)$, and $J_{A_1} = 2/(U + 2J_H)$. Orbital exchange parts are given by

$$\begin{aligned} \hat{A}_{i,i+\hat{x}} &= \sum_{\alpha} t_{\alpha}^2 n_{i\alpha} n_{j\alpha}, \\ \hat{B}_{i,i+\hat{x}} &= \sum_{\alpha < \beta} t_{\alpha} t_{\beta} (\alpha_i^\dagger \beta_i \beta_{i+\hat{x}}^\dagger \alpha_{i+\hat{x}} + \beta_i^\dagger \alpha_i \alpha_{i+\hat{x}}^\dagger \beta_{i+\hat{x}}), \\ \hat{C}_{i,i+\hat{x}} &= \sum_{\alpha < \beta} t_{\alpha} t_{\beta} (\alpha_i^\dagger \beta_i \alpha_{i+\hat{x}}^\dagger \beta_{i+\hat{x}} + \beta_i^\dagger \alpha_i \beta_{i+\hat{x}}^\dagger \alpha_{i+\hat{x}}), \\ \hat{N}_{i,i+\hat{x}} &= \frac{1}{2} \sum_{\alpha, \beta} (t_{\alpha}^2 n_{i\alpha} + t_{\beta}^2 n_{i+\hat{x},\beta}), \end{aligned} \quad (7)$$

where α_i (α_i^\dagger) annihilates (creates) electrons in the α -orbital at i -site. $\mathcal{H}_{\tilde{y}}$ is easily obtained from $\mathcal{H}_{\tilde{x}}$ by switching $t_{\tilde{x}} \leftrightarrow t_{\tilde{y}}$ and replacing $i + \hat{x}$ by $i + \hat{y}$. This Hamiltonian resembles the spin-orbital model describing LaTiO₃ system studied by Khaliullin and his colleagues⁹ in the sense that in LaTiO₃ system, each site has one active electron occupying one of three t_{2g} -orbitals. Yet, there are differences coming from the fact that while our model (6) after the rotation is dealing with three unequal hopping integrals between adjacent orbitals, in LaTiO₃ system the π -hopping is ignored and the other two integrals have equal strengths⁹. By ignoring π -hopping and taking the limit $t + t_2 = t - t_2$ in Eq. (6), our superexchange Hamiltonian becomes identical to that of LaTiO₃. Equations (6) and (7) constitute the main technical findings of the present work.

Some comments about the limiting cases are in order. The exchange Hamiltonian (6) simplifies greatly in the $J_H = 0$ limit,

$$\begin{aligned} \mathcal{H}_{\tilde{x}} &= 4 \sum_i \left(\mathbf{S}_i \cdot \mathbf{S}_{i+\hat{x}} + \frac{1}{4} \right) \sum_{\alpha, \beta} t_{\alpha} t_{\beta} \alpha_i^\dagger \beta_i \beta_{i+\hat{x}}^\dagger \alpha_{i+\hat{x}} \\ &\quad - \sum_{i,\alpha} t_{\alpha}^2 (n_{i\alpha} + n_{i+\hat{x},\alpha}), \\ \mathcal{H}_{\tilde{y}} &= \mathcal{H}_{\tilde{x}} | t_{\tilde{x}} \leftrightarrow t_{\tilde{y}}, i + \hat{x} \rightarrow i + \hat{y} \rangle, \end{aligned} \quad (8)$$

where U is taken to be unity. Furthermore, in the isotropic limit $t_{\tilde{x}} = t_{\tilde{y}} = t_{\tilde{z}}$ the pairwise exchange interaction in Eq. (8) possesses the SU(6) symmetry in the combined spin and orbital spaces¹⁰. The larger symmetry can be most easily seen by defining operators $\Psi_{i,\sigma\alpha} =$

$\varphi_{i\sigma}\alpha_i$ and $\Psi_{i,\sigma\alpha}^\dagger = \alpha_i^\dagger\varphi_{i\sigma}^\dagger$, where $\varphi_{i\sigma}$ ($\varphi_{i\sigma}^\dagger$) annihilates (creates) electrons with spin σ at i -site. The pairwise exchange Hamiltonian can be re-written in the manifestly SU(6)-invariant form $\mathcal{H}_{ij} \sim \sum_{K,K'} \Psi_{j,K}^\dagger \Psi_{i,K} \Psi_{i,K'}^\dagger \Psi_{j,K'}$, where K and K' run over six possible spin and orbital configurations. The SU(6) symmetry will remain for one-dimensional chain consisting of either $\mathcal{H}_{\hat{x}}$ or $\mathcal{H}_{\hat{y}}$ alone, but not for the two-dimensional model $\mathcal{H}_{\hat{x}} + \mathcal{H}_{\hat{y}}$ due to the fact that two different sets of unitary rotations were used to arrive at the overall superexchange Hamiltonian, Eq. (8).

III. ORBITAL DM AND PHASE DIAGRAM

In this section we explicitly point out the emergence of DM-type orbital exchange interaction in our model and

study possible phase diagram using the site-factorization scheme. DM-type interactions will be recovered by unrotating the Hamiltonian (7) to the original orbital basis as shown in Ref. 8. In doing so for our Hamiltonian (6) one encounters unwieldy expressions that simplify somewhat by taking the weaker π -bonding to zero: $t_b = 0$. This limit is usually taken in the superexchange calculation for d -orbital systems in transition metal oxides⁹, and more recently for p -orbital systems in an optical lattice¹¹.

In such limit the orbital exchange operators in Eq. (7) can be re-expressed in terms of Gell-Mann matrices λ^α ($\alpha = 1 \dots 8$) as follows:

$$\begin{aligned}
\mathcal{H}_{\hat{x}} = & \frac{J_{T_1}}{4} \sum_i \left(\mathbf{s}_i \cdot \mathbf{s}_{i+\hat{x}} + \frac{3}{4} \right) \left(t_{\bar{X}}^2 [\lambda_i^x + (\lambda_i^x)^2] [\lambda_{i+\hat{x}}^x + (\lambda_{i+\hat{x}}^x)^2] + t_{\bar{Z}}^2 [-\lambda_i^x + (\lambda_i^x)^2] [-\lambda_{i+\hat{x}}^x + (\lambda_{i+\hat{x}}^x)^2] \right. \\
& \left. + 2t_{\bar{X}}t_{\bar{Z}} [\lambda_i^4 \lambda_{i+\hat{x}}^4 + \lambda_i^5 \lambda_{i+\hat{x}}^5] \right) \\
& - \frac{J_E}{4} \sum_i \left(\mathbf{s}_i \cdot \mathbf{s}_{i+\hat{x}} - \frac{1}{4} \right) \left(t_{\bar{X}}^2 [\lambda_i^x + (\lambda_i^x)^2] [\lambda_{i+\hat{x}}^x + (\lambda_{i+\hat{x}}^x)^2] + t_{\bar{Z}}^2 [-\lambda_i^x + (\lambda_i^x)^2] [-\lambda_{i+\hat{x}}^x + (\lambda_{i+\hat{x}}^x)^2] \right. \\
& \left. - 2t_{\bar{X}}t_{\bar{Z}} [\lambda_i^4 \lambda_{i+\hat{x}}^4 + \lambda_i^5 \lambda_{i+\hat{x}}^5] \right) \\
& + \frac{J_{A_1}}{3} \sum_i \left(\mathbf{s}_i \cdot \mathbf{s}_{i+\hat{x}} - \frac{1}{4} \right) \left(\frac{1}{2} t_{\bar{X}}^2 [\lambda_i^x + (\lambda_i^x)^2] [\lambda_{i+\hat{x}}^x + (\lambda_{i+\hat{x}}^x)^2] + \frac{1}{2} t_{\bar{Z}}^2 [-\lambda_i^x + (\lambda_i^x)^2] [-\lambda_{i+\hat{x}}^x + (\lambda_{i+\hat{x}}^x)^2] \right. \\
& \left. + t_{\bar{X}}t_{\bar{Z}} [\lambda_i^4 \lambda_{i+\hat{x}}^4 - \lambda_i^5 \lambda_{i+\hat{x}}^5] \right) \\
& + \frac{J_{T_2}}{3} \sum_i \left(\mathbf{s}_i \cdot \mathbf{s}_{i+\hat{x}} - \frac{1}{4} \right) \left(t_{\bar{X}}^2 [\lambda_i^x + (\lambda_i^x)^2] [\lambda_{i+\hat{x}}^x + (\lambda_{i+\hat{x}}^x)^2] + t_{\bar{Z}}^2 [-\lambda_i^x + (\lambda_i^x)^2] [-\lambda_{i+\hat{x}}^x + (\lambda_{i+\hat{x}}^x)^2] \right. \\
& \left. - t_{\bar{X}}t_{\bar{Z}} [\lambda_i^4 \lambda_{i+\hat{x}}^4 - \lambda_i^5 \lambda_{i+\hat{x}}^5] \right) \\
& - t_{\bar{X}}^2 (n_{i,\bar{X}} + n_{i+\hat{x},\bar{X}}) - t_{\bar{Z}}^2 (n_{i,\bar{Z}} + n_{i+\hat{x},\bar{Z}}), \\
\mathcal{H}_{\hat{y}} = & \mathcal{H}_{\hat{x}} | (t_{\bar{X}} \rightarrow t_{\bar{Y}}, \lambda^x \rightarrow \lambda^y, \lambda^4 \rightarrow \lambda^6, \lambda^5 \rightarrow \lambda^7, i+\hat{x} \rightarrow i+\hat{y}, n_{i,\bar{X}} \rightarrow n_{i,\bar{Y}}, n_{i+\hat{x},\bar{X}} \rightarrow n_{i+\hat{y},\bar{Y}}). \tag{9}
\end{aligned}$$

For convenience we introduced $\lambda^x = \text{diag}(1, 0, -1)$ and $\lambda^y = \text{diag}(0, 1, -1)$ as combinations of λ^3 , λ^8 and the unit matrix. It is useful to note that $\mathcal{H}_{\hat{x}}$ is entirely constructed from three matrices, $\mathbf{T}_i^x = (\lambda_i^4, \lambda_i^5, \lambda_i^x)$, reducing to a set of Pauli matrices in the orbital subspace of (p_x, p_z) . Similarly, $\mathcal{H}_{\hat{y}}$ employs another set of three matrices and $\mathbf{T}_i^y = (\lambda_i^6, \lambda_i^7, \lambda_i^y)$ reducing to Pauli matrices in the (p_y, p_z) orbital subspace.

Returning to the original basis (p_x, p_y, p_z) amounts to making the unitary replacements

$$\begin{aligned}
(\lambda_i^\alpha, \lambda_{i+\hat{x}}^\alpha) & \rightarrow (U_x \lambda_i^\alpha U_x^\dagger, U_x^\dagger \lambda_{i+\hat{x}}^\alpha U_x), \\
(\lambda_i^\alpha, \lambda_{i+\hat{y}}^\alpha) & \rightarrow (U_y \lambda_i^\alpha U_y^\dagger, U_y^\dagger \lambda_{i+\hat{y}}^\alpha U_y), \tag{10}
\end{aligned}$$

in Eq. (9). After the rotation there appear terms linear in γ ,

$$\begin{aligned}
t\gamma \sum_i & \left([\lambda_i^x + (\lambda_i^x)^2] \lambda_{i+\hat{x}}^4 - \lambda_i^4 [\lambda_{i+\hat{x}}^x + (\lambda_{i+\hat{x}}^x)^2] \right. \\
& \left. + [\lambda_i^y + (\lambda_i^y)^2] \lambda_{i+\hat{y}}^6 - \lambda_i^6 [\lambda_{i+\hat{y}}^y + (\lambda_{i+\hat{y}}^y)^2] \right). \tag{11}
\end{aligned}$$

As mentioned earlier, $(\lambda^4, \lambda^5, \lambda^x)$ are effectively replaced

by the Pauli matrices $\boldsymbol{\tau} = (\tau^x, \tau^y, \tau^z)$ within the (p_x, p_z) -orbital subspace, thus the first line of Eq. (11) becomes

$$t\gamma \sum_i [\tau_i^z \tau_{i+\hat{x}}^x - \tau_i^x \tau_{i+\hat{x}}^z] = t\gamma \sum_i \hat{y} \cdot [\boldsymbol{\tau}_i \times \boldsymbol{\tau}_{i+\hat{x}}]. \quad (12)$$

This is the orbital analogue of the DM spin exchange, or ‘‘orbital DM’’ (ODM) exchange. The real-valued transition amplitudes obtained from the superexchange process necessarily excludes the imaginary τ_y operator, permitting $\hat{y} \cdot [\boldsymbol{\tau}_i \times \boldsymbol{\tau}_{i+\hat{x}}]$ as the only permissible form of DM interaction. Analogously, the second line of Eq. (11) reduces to the two-component (p_y, p_z) -orbital model with $(\lambda^6, \lambda^7, \lambda^y)$ acting as another set of Pauli matrices $\boldsymbol{\mu}$ with the DM interaction, $2t\gamma \sum_i \hat{y} \cdot [\boldsymbol{\mu}_i \times \boldsymbol{\mu}_{i+\hat{y}}]$. We emphasize that such Pauli matrix description (effective spin-1/2 model) must give way to the full Gell-Mann matrix formalism shown in Eq. (9) once $\mathcal{H}_{\hat{x}}$ and $\mathcal{H}_{\hat{y}}$ are combined in the two-dimensional lattice.

A similar Gell-Mann matrix expression appeared in the

low-energy theory of hard-core three-component bosons confined in the optical lattice¹¹ where, however, the influence of ISB on the superexchange process was not examined. Superexchange calculation for the t_{2g} -orbitals in the presence of GdFeO₃-type distortion was carried out by Ishihara *et al.*¹². The oxygen distortions assumed in their work is staggered, in the sense that the net displacement vector of all the oxygen atoms is zero. On the contrary, we are dealing with the situation where displacement of the p_z is uniform, due to external fields. Orbital analogue of the DM exchange as shown here might be anticipated on symmetry grounds, but has never been explicitly demonstrated before.

In proceeding to the mean-field analysis of the possible phases of our Hamiltonian we assume that J_H is sufficiently large to favor the ferromagnetic spin state⁹, $\langle \mathbf{S}_i \cdot \mathbf{S}_j \rangle = 1/4$. The approximation allows us to focus on the orbital sector, which makes Eq. (9) simple enough to be written down in original basis $\psi_i = (X_i \ Y_i \ Z_i)^T$ as

$$\begin{aligned} \mathcal{H}_{\hat{x}} &= 2t^2 \sum_i [\lambda_i^x + (\lambda_i^x)^2 - 1][\lambda_{i+\hat{x}}^x + (\lambda_{i+\hat{x}}^x)^2 - 1] + 2t\gamma \sum_i \left([\lambda_i^x + (\lambda_i^x)^2] \lambda_{i+\hat{x}}^4 - \lambda_i^4 [\lambda_{i+\hat{x}}^x + (\lambda_{i+\hat{x}}^x)^2] \right) \\ &\quad + \gamma^2 \sum_i \left(\lambda_i^5 \lambda_{i+\hat{x}}^5 - \lambda_i^4 \lambda_{i+\hat{x}}^4 - \lambda_i^x \lambda_{i+\hat{x}}^x + [(\lambda_i^x)^2 - 1][(\lambda_{i+\hat{x}}^x)^2 - 1] \right), \\ \mathcal{H}_{\hat{y}} &= 2t^2 \sum_i [\lambda_i^y + (\lambda_i^y)^2 - 1][\lambda_{i+\hat{y}}^y + (\lambda_{i+\hat{y}}^y)^2 - 1] + 2t\gamma \sum_i \left([\lambda_i^y + (\lambda_i^y)^2] \lambda_{i+\hat{y}}^6 - \lambda_i^6 [\lambda_{i+\hat{y}}^y + (\lambda_{i+\hat{y}}^y)^2] \right) \\ &\quad + \gamma^2 \sum_i \left(\lambda_i^7 \lambda_{i+\hat{y}}^7 - \lambda_i^6 \lambda_{i+\hat{y}}^6 - \lambda_i^y \lambda_{i+\hat{y}}^y + [(\lambda_i^y)^2 - 1][(\lambda_{i+\hat{y}}^y)^2 - 1] \right), \end{aligned} \quad (13)$$

where $U - 3J_H$ is taken to be unity and $t \equiv t_a/2$ for brevity. The Hamiltonian (13) is replaced by its mean-field form by making the on-site ansatz of the wave function,

$$|\psi_i\rangle = A_i^x |X_i\rangle + A_i^y |Y_i\rangle + A_i^z |Z_i\rangle, \quad (14)$$

with three complex coefficients satisfying $|A_i^x|^2 + |A_i^y|^2 + |A_i^z|^2 = 1$. The many-body wave function becomes the direct product $|\psi\rangle = \prod_i \otimes |\psi_i\rangle$, and one can make replacement of the operator λ_i^α with its average, $\langle \lambda_i^\alpha \rangle$, in the Hamiltonian. In this scheme one can choose A_i^x real without loss of generality and parameterize the coefficients generally as $A_i^x = \cos \alpha_i$, $A_i^y = e^{i\gamma_i} \sin \alpha_i \cos \beta_i$, $A_i^z = e^{i\delta_i} \sin \alpha_i \sin \beta_i$. The mean-field Hamiltonian being a function of the four angles $(\alpha_i, \beta_i, \gamma_i, \delta_i)$ per site can be minimized by the Monte Carlo (MC) annealing method. We may enrich the phase diagram of the model somewhat by introducing one more parameter A to replace $t\gamma \rightarrow tA\gamma$. Various renormalization of the interaction parameters may alter the coefficients in the superexchange

Hamiltonian from those shown in Eq. (6), which we attempt to model with the extra parameter A . It is also an attempt to understand the possible phases of the orbital DM model within the wider perspective than might be allowed from second-order perturbation.

The zero-temperature phase diagram spanned by (γ, A) with t fixed to unity is shown in Fig. 1. Six Gell-Mann matrices, organized into two groups $\mathbf{T}_i^x = (\lambda_i^4, \lambda_i^5, \lambda_i^x)$ and $\mathbf{T}_i^y = (\lambda_i^6, \lambda_i^7, \lambda_i^y)$, are used to characterize the ground states by following their averages and their Fourier components: $\mathbf{T}_{\mathbf{k}}^n = \sum_i \langle \mathbf{T}_i^n \rangle e^{-i\mathbf{k} \cdot \mathbf{r}_i}$ ($n = x, y$). The Fourier analysis is particularly helpful in searching for modulated structures with long periods that often appear with the DM interaction.

When $\gamma = 0$ the Hamiltonian is expressed entirely in terms of two commuting matrices, $(\lambda_i^x, \lambda_i^y)$, with the ground state given by alternate occupations of p_x and p_y orbitals on the square lattice. This phase, called the antiferro-orbital (AFO) state, dominates the small- γ region of the phase diagram. For A small and γ increasing beyond a critical value, one finds a first-order transition into a ferro-orbital (FO) state with p_z -orbital oc-

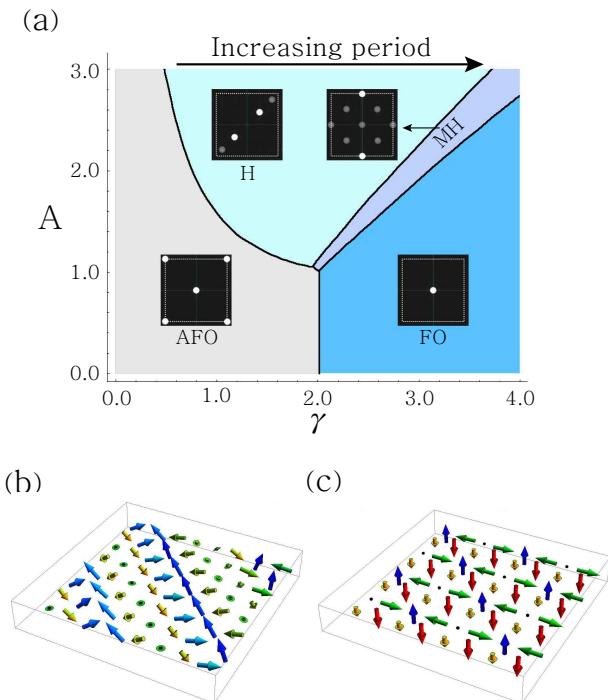


FIG. 1: (color online) (a) Zero-temperature phase diagram of the recovered orbital model in Eq. (13) with $t = 1$. Phase boundaries are obtained on the basis of MC simulation and variational energy calculation. Orbital configurations are abbreviated as AFO (antiferro-orbital), FO (ferro-orbital), H (helical), and MH (multiple helical). Bragg patterns for each phase are schematically shown with dotted line denoting the first Brillouin zone boundary. In H, the period increases continuously as γ becomes larger. Bragg spots at (k, k) and $(3k, 3k)$ are both present in H. Real space spin configurations in terms of $\langle \mathbf{T}_i^x \rangle$ for (b) H and (c) MH phases are depicted.

cupation at every site. In the phase diagram of Fig. 1 one finds that we are considering rather large γ values. While this may be unlikely in conventional solid materials, a thin film consisting of narrow-band materials subject to very large perpendicular electric field may be able to realize such physical regime. Inhabiting the large- A , intermediate- γ region is the $\langle 11 \rangle$ helical (H) phase that we found to be well described by

$$\begin{aligned} \langle \mathbf{T}_i^x \rangle &= \left(\sin 2[\mathbf{k} \cdot \mathbf{r}_i + \alpha_0] \sin[\mathbf{k} \cdot \mathbf{r}_i + \beta_0], 0, \right. \\ &\quad \left. \cos^2[\mathbf{k} \cdot \mathbf{r}_i + \alpha_0] - \sin^2[\mathbf{k} \cdot \mathbf{r}_i + \alpha_0] \sin^2[\mathbf{k} \cdot \mathbf{r}_i + \beta_0] \right), \\ \langle \mathbf{T}_i^y \rangle &= \left(\sin^2[\mathbf{k} \cdot \mathbf{r}_i + \alpha_0] \sin 2[\mathbf{k} \cdot \mathbf{r}_i + \beta_0], 0, \right. \\ &\quad \left. \sin^2[\mathbf{k} \cdot \mathbf{r}_i + \alpha_0] \cos 2[\mathbf{k} \cdot \mathbf{r}_i + \beta_0] \right), \end{aligned} \quad (15)$$

$\mathbf{k} = (k, k)$. Variational calculation of the minimum energy with respect to k and the relative phase angle $\alpha_0 - \beta_0$ confirms that the period $2\pi/k$ is increased with γ , 2 on the smaller γ side to > 6 , before it is supplanted by another intricate phase taking place between H and FO.

The emergence of orbital spiral phase is a natural consequence of the orbital DM exchange.

The new phase, indicated as MH in Fig. 1, is constructed as the equal-weight superposition of two helices with $\mathbf{k}_1 = \pm(\pi/2, \pi/2)$ and $\mathbf{k}_2 = \pm(\pi/2, -\pi/2)$, as well as two pairs of peaks at $\pm(\pi, 0)$ and $\pm(0, \pi)$. The intensities obtained from Fourier analysis of $\langle \mathbf{T}_i^x \rangle$ (inset in Fig. 1) show stronger peaks at $\pm(0, \pi)$ than at $\pm(\pi, 0)$. On the other hand Fourier analysis of $\langle \mathbf{T}_i^y \rangle$ revealed the Bragg peaks at $\pm(\pi, 0)$ are brighter than at $\pm(0, \pi)$. One can still draw a close parallel of the MH phase found in the present model to the square lattice of Skyrmions and anti-Skyrmions found in some models of spiral magnetism^{14,15}, which also consists of multiple Bragg peaks at $\pm(k, k)$ and $\pm(k, -k)$ in its spin structure.

IV. CONCLUSION AND SUMMARY

Orbital ordering in multi-band Hubbard systems have been studied for several decades since the pioneering work of Kugel and Khomskii (KK)¹³. Extension of the original two-orbital KK model to three-orbital t_{2g} case has been thoroughly carried out by Khaliullin and collaborators⁹. Recent works on the optical lattice of cold atoms also arrived at three-orbital exchange model¹¹, without the spin degrees of freedom. Meanwhile, remarkable advances in the growth technique of ultrathin materials prompt consideration of the influence of ISB, $\gamma \neq 0$, on the electronic band structure and, as we discuss in this paper, on the orbital physics as well. With this background, we have derived the analogue of spin-DM exchange interaction as a natural consequence of ISB in the multi-orbital Hubbard model. Physical requirements for its appearance are the multi-orbital degeneracy and the loss of inversion symmetry, but not the spin-orbit interaction as in the spin-DM exchange.

Although the derivations presented in this paper are based on the p -orbital picture, the case of degenerate t_{2g} -orbitals with ISB can be worked out, without further calculation, by making the replacements $(p_x, p_y, p_z) \rightarrow (d_{yz}, d_{zx}, d_{xy})$, and switching $\sigma \leftrightarrow \pi$ -hopping integrals $t_a \leftrightarrow t_b$ in all our results. It is thus expected that conclusions regarding the phase diagram as shown in Fig. 1 may be directly applicable to ultra-thin films made of transition-metal elements. Unlike the spin-DM interaction in materials, the governing factor γ responsible for the orbital-DM exchange can be imposed externally by the electric field in a controlled manner. Interesting quantum-orbital phases and transitions between them may be observed in a thin-film multi-orbital system subject to perpendicular electric field of variable strength.

Acknowledgments

J. H. H. is supported by NRF grant (No. 2011-0015631). P. K. is supported by NRF grant funded by the

Korean Government (NRF-2012) - Global Ph. D. Fellowship Program. Insightful comments from Giniyat Khali-

ullin and Hosho Katsura are gratefully acknowledged.

* Electronic address: hanjh@skku.edu

- ¹ P. W. Anderson, *Phys. Rev.* **79**, 350 (1950).
- ² I. E. Dzyaloshinskii, *J. Chem. Solids* **4**, 241 (1958); T. Moriya, *Phys. Rev.* **120**, 91 (1960); *Phys. Rev. Lett.* **4**, 228 (1960).
- ³ Y. A. Bychkov and E. I. Rashba, *JETP Lett.* **39**, 78 (1984).
- ⁴ L. Petersen and P. Hedegård, *Surf. Sci.* **459**, 49 (2000).
- ⁵ Jin-Hong Park, Choong H. Kim, Jun-Won Rhim, and Jung Hoon Han, *Phys. Rev. B* **85**, 195401 (2012).
- ⁶ Beomyoung Kim, Choong H. Kim, Panjin Kim, Wonsig Jung, Yeongkwan Kim, Yoonyoung Koh, Masashi Arita, Kenya Shimada, Hirofumi Namatame, Masaki Taniguchi, Jaejun Yu, and Changyoung Kim, *Phys. Rev. B* **85**, 195402 (2012).
- ⁷ A. M. Oleś, *Phys. Rev. B* **28**, 327 (1983).
- ⁸ L. Shekhtman, O. Entin-Wohlman, and Amnon Aharony, *Phys. Rev. Lett.* **69**, 836 (1992).
- ⁹ G. Khaliullin and S. Maekawa, *Phys. Rev. Lett.* **85**, 3950 (2000); G. Khaliullin and S. Okamoto, *Phys. Rev. B* **68**, 205109 (2003); G. Khaliullin, *Prog. Theor. Phys. Suppl.* **160**, 155 (2005).
- ¹⁰ Daniel P. Arovas and Assa Auerbach, *Phys. Rev. B* **52**, 10114 (1995); Y. Q. Li, M. Ma, D. N. Shi, and F. C. Zhang, *Phys. Rev. Lett.* **81**, 3527 (1998); Y. Yamashita, N. Shibata, and K. Ueda, *Phys. Rev. B* **58**, 9114 (1998); Swapan K. Pati, Rajiv R. P. Singh, and Daniel I. Khomskii, *Phys. Rev. Lett.* **81**, 5406 (1998).
- ¹¹ Philipp Hauke, Erhai Zhao, Krittika Goyal, Ivan H. Deutsch, W. Vincent Liu, and Maciej Lewenstein, *Phys. Rev. A* **84**, 051603(R) (2011).
- ¹² S. Ishihara, T. Hatakeyama, and S. Maekawa, *Phys. Rev. B* **65**, 064442 (2002).
- ¹³ K. I. Kugel and D. I. Khomskii, *Sov. Phys. Usp.* **25**, 231 (1982).
- ¹⁴ U. K. Roßler, A. N. Bogdanov, and C. Pfleiderer, *Nature* **442**, 797 (2006).
- ¹⁵ Su Do Yi, Shigeki Onoda, Naoto Nagaosa, and Jung Hoon Han, *Phys. Rev. B* **80**, 054416 (2009).